Available online at www.sciencedirect.com
ScienceDirect
Chemical Physics 333 (2007) 236–245
Chemical Physics
www.elsevier.com/locate/chemphys

Structural study of two reactive diacetylenes

Sylvie Spagnoli [a,*], Michel Schott [b], Mark Johnson [c], Loic Toupet [d]

[a] Laboratoire de Spectrométrie Physique UMR 5588-CNRS, Université Joseph Fourier, BP87, 38402 Saint Martin d'Hères, France
[b] Institut des Nanosciences de Paris UMR 7588-CNRS, Université Pierre et Marie Curie-Paris 6, et Université Denis Diderot-Paris 7, Campus Boucicaut, 140 rue de Lourmel, 75015, Paris, France
[c] Institut Laue-Langevin, 6, Rue Jules Horowitz, BP 156, 38042 Grenoble Cedex 9, France
[d] Groupe Matière Condensée et Matériaux, UMR 6626-CNRS, Université de Rennes I, Campus de Beaulieu, 35042 Rennes Cedex, France

Received 25 October 2006; accepted 7 February 2007
Available online 15 February 2007

Abstract

The unit cell dimensions of two diacetylenes 3BCMU and 4BCMU are measured from low temperature to 300 K. The complete crystal structures of the two phases of 3BCMU are determined at 110 K by X-ray diffraction and at 270 K by neutron diffraction helped by calculated geometrical optimization used as a starting structure. Neutron results allow to discuss the hydrogen bond strength and to determine the thermal expansion coefficients.

Keywords: Diacetylene crystals; Reactive monomers; Crystal structure; Hydrogen bond

1. Introduction

Isolated polydiacetylene (PDA) chains dispersed in their single crystal monomer matrix have been used as model systems for the study of spectroscopic properties of conjugated polymers, since they are close to the theoretical model of a linear, regular and very long conjugated chain [1]. This system can be obtained thanks to the special polymerization mechanism of DA [2], which is a topochemical reaction [3] in the monomer crystal (Scheme 1). According to models of the reaction, maximal reactivity is expected for $d \approx 5$ Å and $\gamma \approx 45°$ [4,5].

The general formula of PDA is $=(R–C–C\equiv C–C–R')_n=$ where R and R′ are side groups, which may be different or identical, and may have very diverse chemical structures.

Knowledge of monomer crystal structures is important for two reasons. The structure governs the topochemical reaction (usually performed at room temperature); it also governs the geometry of isolated polymer chains in the monomer matrix, the periodic potential in which they are embedded, and hence their spectroscopic properties (usually studied a low temperature).

The conditions to obtain isolated chains behaving as perfect quantum wires [1,6–18] are met in the reactive DA known as 3 and 4 BCMU which are studied in the present work. Their side-group formulae are $R = R' = –(CH_2)_n–OCONH–CH_2–COOC_4H_9$ with $n = 3$ or 4 for 3BCMU and 4BCMU, respectively.

4BCMU and 3BCMU monomer crystals polymerize very rapidly under γ or X-ray irradiation at room temperature [8,19], and down to 200 K at least. Structural studies in that temperature range can only be performed by neutron diffraction. At low enough temperature, chain propagation in DA crystals becomes blocked [20]; this allowed a few low temperature structures to be obtained using X-rays [5,21–23].

In the present paper the temperature dependence of the unit cells of 3 and 4 BCMU monomer crystals has been determined using neutron diffraction. To obtain the 3 BCMU crystallographic structure in its two phases at 110 K and 270 K, different methods have been used, X-rays diffraction at 110 K, neutron diffraction at 270 K helped by a calculated geometrical optimisation.

* Corresponding author. Tel.: +33 4 76 51 47 85; fax: +33 4 76 63 54 95.
E-mail address: sylvie.spagnoli@ujf-grenoble.fr (S. Spagnoli).

0301-0104/$ - see front matter © 2007 Elsevier B.V. All rights reserved.
doi:10.1016/j.chemphys.2007.02.007

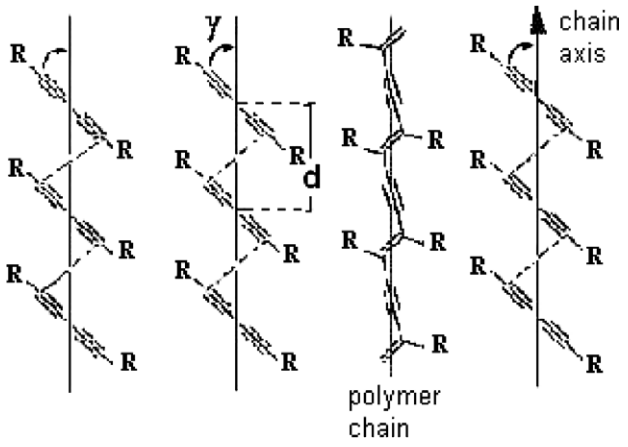

Scheme 1. Topochemical DA polymerization.

Using these structure, two problems are addressed in the following two companion papers: photopolymerization in [24] and the effect of strain on the spectroscopic properties of isolated chains in [25].

2. Experimental section

2.1. Neutron diffraction

Structures were studied on the neutron diffractometer D19 at Institut Laue Langevin, Grenoble, France [26] using a wavelength of 1.538 Å and the associated software. In this instrument, there is a very low γ-ray background, mainly due to nuclear reactions of thermal neutrons with aluminium parts of the apparatus. The H(n,γ)D reaction with a cross-section of 0.333 barn, which produces 2.2 MeV photons, also contributes somewhat to irradiation of the studied sample. A rough estimate leads to a dose of 10–20 rad/day, which is enough to produce at the end of the experiment a polymer content of the order of 1 to 2% in weight. A final polymer content of 1% was measured by absorption spectroscopy using calibration of Ref. [8]. It was checked that such polymer content does not significantly change the unit cell parameters.

A drawback of neutron diffraction is the small scattering power, so that relatively large crystals are required. Several crystals were used, with typical dimensions $5 \times 5 \times 0.2$ mm. As shown bellow, the studied materials are lamellar, and single crystals of that size are not easily grown. Crystals were obtained by slow evaporation of acetone solutions at 4 °C in the dark.

2.2. X-ray diffraction

The samples (typically: $0.45 * 0.35 * 0.22$ mm) were studied on a NONIUS Kappa CCD with Graphite monochromatized MoKα ($\lambda = 0.71073$ A) radiation. The cell parameters were obtained with Denzo and Scalepack [27] with 10 frames (psi rotation: 1° per frame). The data collection [28] ($2\theta_{max} = 54°$, 1327 frames via 0.3° omega rotation and 6 s per frame, *hkl* range: *h* 0,7 6; *k* 0,6; l −1 1, 1 1) gave 62286 reflections. The data reduction led to 2438 independent reflections from which 1936 with $I > 2.0\sigma(I)$ [27]. The structure was solved with SIR-97 [29] which reveals the non-hydrogen atoms of the molecule. After anisotropic refinement, many hydrogen atoms can be found by Fourier difference. The whole structure was refined with SHELXL97 [30] by the full-matrix least-square technique (use of F square magnitude; x,y,z, β_{ij} for C, O and N atoms, x,y,z in riding mode for H atoms; 158 variables and 1936 observations with $I > 2.0\sigma(I)$; calc $w = 1/[\sigma^2(Fo^2) + (0.055\ P)^2 + 3.53\ P]$ where $P = (Fo^2 + 2Fc^2)/3$ with the resulting $R = 0.048$, $R_w = 0.116$ and $S_w = 1.029$, $\Delta\rho$ 0.2 eÅ^{-3}). Atomic scattering factors are taken from International tables for X-ray crystallography [31].

2.3. Differential scanning calorimetry (DSC)

Measurements were performed on a Perkin Elmer DSC 7 with a 10 K/min heating rate.

3. 3BCMU monomer

3.1. Calorimetric detection of a solid–solid phase transition

The 3BCMU monomer crystal undergoes a first order phase transition near 155 K, which was studied using DSC. Scans were performed between 110 and 300 K at heating or cooling rate of 10 K/min. For extrapolation to zero heating/cooling rate, it was assumed that the measured transition temperature varied with rate as it does in 4BCMU [1]. The transition temperature extrapolated in that way is 156 K on cooling and 161.5 K on heating in samples with a very small polymer content (less than 10^{-4} in weight), so an hysteresis of 5.5 K. The transition enthalpy is 3.6 ± 0.12 J/g, very similar to the value found at 226 K in 4BCMU [1].

3.2. Room temperature phase II and temperature dependence

At 270 K the structure is monoclinic with $a = 59.748(3)$ Å, $b = 4.8776(3)$ Å, $c = 9.0472(5)$ Å, $\beta = 90.300(5)°$, $V = 2636.6(3)$ Å^3, $Z = 4$, proposed group C2/c (no. 15). The structure is clearly monoclinic, despite a β angle close to 90°. This is shown by the observed extinctions and by the fact that orthorhombic refinements lead to large errors.

A set of 778 non-zero independent reflections was collected. Since the asymmetric unit contains 35 atoms, including the hydrogens, there are too many parameters to directly refine the atomic positions. The structure was therefore obtained in two steps. First, a structure was determined at 110 K using X-rays (see below). The resulting atomic positions were then used to find a force field preserving the experimental structure during geometry optimization, namely COMPASS in Materials Studio program suite from Accelrys [32]. This force field was then

Table 1
Final atomic parameters of 3BCMU monomer for non-H atoms at 110 K and 270 K

110 K				270 K			
Atom	*x/a*	*y/b*	*z/c*	Atom	*x/a*	*y/b*	*z/c*
C1	5066(1)	4053(4)	438(2)	C1	5069(4)	4043(17)	322(13)
C2	5181(1)	2402(4)	1197(2)	C2	5180(4)	2490(15)	1050(3)
C3	5319(1)	450(4)	2182(2)	C3	5313(5)	560(8)	1970(3)
C4	5501(1)	1870(4)	3297(2)	C4	5494(4)	1990(6)	2920(3)
C5	5677(1)	3440(4)	2561(2)	C5	5661(5)	3510(6)	1900(3)
O1	5799(1)	1475(2)	1755(1)	O1	5781(5)	1490(7)	1050(4)
O2	6013(1)	5002(3)	1045(2)	O2	5981(6)	5080(9)	140(4)
O3	6507(1)	1557(3)	1943(1)	O3	6476(5)	1480(8)	700(4)
O4	6592(1)	4320(3)	84(1)	O4	6567(5)	4150(9)	−1250(4)
N1	6071(1)	642(3)	290(2)	N1	6049(3)	770(6)	−640(2)
C6	5966(1)	2559(4)	1035(2)	C6	5948(4)	2660(16)	180(3)
C7	6264(1)	1474(4)	−446(2)	C7	6240(5)	1520(7)	−1590(3)
C8	6463(1)	2431(4)	680(2)	C8	6437(4)	2650(16)	−530(3)
C9	6781(1)	5381(4)	1123(2)	C9	6767(5)	5150(7)	−380(3)
C10	6925(1)	7248(4)	281(2)	C10	6904(5)	6760(6)	−1360(3)
C11	7127(1)	8356(4)	1346(2)	C11	7114(4)	−7940(8)	460(3)
C12	7282(1)	10258(5)	589(3)	C12	7275(5)	9330(7)	−1370(3)

The values given are fractional coordinates ($\times 10^4$); e.s.d.'s are given in parentheses.

used to optimize atomic positions in the high T unit cell, starting from fractional coordinates from the experimental low T structure. The result was imported in XTAL [33] as a starting point for structure refinement from experimental neutron data at 270 K.

Atomic positions are given in Table 1, and bond lengths and angles in Tables 2 and 3. Atomic labelling is shown in Scheme 2. An ORTEP [34] view of the 3BCMU packing in the [0 1 0] plane is shown in Scheme 3. Compared to Scheme 1, the 3BCMU geometry is favourable for polymerisation, since $\gamma = 50°$ and $d = 4.878$ Å.

The filling factor, calculated by PLATON [35], is 0.68 at 270 K, a value commonly found in molecular crystals [36].

For the determination of thermal expansion, a smaller number (30–40) reflections were collected at several other

Table 2
3BCMU molecular bond lengths (Å) at 110 K and 270 K

110 K		270 K	
C1–C2	1.200(3)	C1–C2	1.20(5)
C1–C1	1.382(4)	C1–C1	1.38(2)
C2–C3	1.466(3)	C2–C3	1.48(6)
C3–C4	1.528(3)	C3–C4	1.55(4)
C4–C5	1.507(3)	C4–C5	1.55(4)
O1–C5	1.446(2)	C5–O1	1.44(4)
O1–C6	1.350(2)	O1–C6	1.39(5)
O2–C6	1.220(2)	O2–C6	1.20(9)
O3–C8	1.204(2)	O3–C8	1.28(5)
O4–C8	1.344(2)	O4–C8	1.25(6)
O4–C9	1.446(2)	O4–C9	1.51(5)
N1–H1	0.86(3)	N1–H1	1.06(7)
N1–C6	1.341(2)	N1–C6	1.33(6)
N1–C7	1.444(2)	N1–C7	1.48(4)
C7–C8	1.513(3)	C7–C8	1.61(4)
C9–C10	1.510(2)	C9–C10	1.44(4)
C10–C11	1.519(3)	C10–C11	1.60(4)
C11–C12	1.522(3)	C11–C12	1.44(4)

Table 3
3BCMU molecular angles (degrees) at 110 K and 270 K

110 K		270 K	
C2–C1–C1	179.7(3)	C2–C1–C1	172(2)
C1–C2–C3	177.6(2)	C1–C2–C3	179(3)
C2–C3–C4	112.55(17)	C2–C3–C4	113(3)
C5–C4–C3	113.86(14)	C3–C4–C5	110(2)
O1–C5–C4	107.39(15)	C4–C5–O1	108(3)
C6–O1–C5	114.85(14)	C5–O1–C6	113(4)
C8–O4–C9	114.35(13)	C8–O4–C9	114(3)
C6–N1–C7	118.05(15)	C6–N1–C7	121(3)
O2–C6–O1	123.52(16)	O1–C6–O2	122(4)
N1–C6–O1	111.95(15)	O1–C6–N1	111(6)
O2–C6–N1	124.52(16)	O2–C6– N1	126(3)
N1–C7–C8	111.47(14)	N1–C7–C8	107(2)
O3–C8–O4	123.68(17)	O3–C8–O4	127(3)
O3–C8–C7	124.54(17)	O3–C8–C7	120(5)
O4–C8–C7	111.74(14)	O4–C8–C7	110(3)
O4–C9–C10	109.11(14)	O4–C9–C10	108(3)
C9–C10–C11	110.10(14)	C9–C10–C11	109(2)
C10–C11–C12	113.69(16)	C10–C11–C12	114(2)

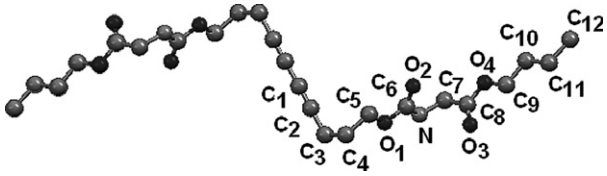

Scheme 2. ORTEP view of the 3BCMU molecule with atomic labeling.

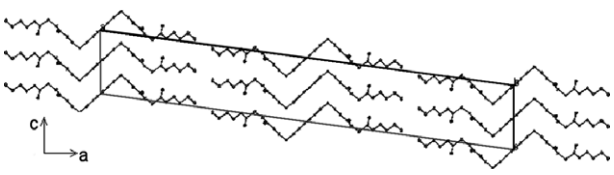

Scheme 3. ORTEP view of the 3BCMU molecules projection on the [0 1 0] plane.

Table 4
3BCMU temperature dependence of lattice parameters

Temperature (K)	a (Å)	b (Å)	c (Å)	β (°)	V (Å^3)
270	59.641(14)	4.8770(9)	9.0413(17)	90.25(2)	2630(2)
260	59.722(50)	4.8733(11)	9.0378(44)	90.26(5)	2630(5)
250	59.693(31)	4.8716(14)	9.0307(26)	90.28(3)	2626(3)
185	59.453(75)	4.8621(35)	8.988(83)	90.18(9)	2598(8)
154	58.854(13)	4.8645(6)	8.9795(11)	92.964(15)	2567(1)
140	58.74(14)	4.875(5)	8.971(8)	94.60(13)	2603(1)
135	58.749(61)	4.8717(28)	8.962(6)	94.11(7)	2558(6)
120	58.7043(2)	4.872(5)	8.9550(5)	97.614(2)	2539(3)
110	58.715(2)	4.8687(2)	8.9578(3)	97.593(1)	2538(0)
93	58.6067(15)	4.8578(1)	8.9431(3)	97.5912(11)	2524(0)

temperatures. The corresponding lattice parameters are given in Table 4, and their temperature dependence is shown in Fig. 1a–e. The thermal expansion coefficients are:

in the a direction $\alpha_a = 6 \pm 2 \times 10^{-5}$ K^{-1},
in the b direction $\alpha_b = 3.7 \pm 0.3 \times 10^{-5}$ K^{-1},
in the c direction $\alpha_c = 6 \pm 2 \times 10^{-5}$ K^{-1}.

3.3. Low temperature phase

The parameters found for phase II are quite different from those obtained by Enkelmann at 110 K, using X-ray diffraction: $a = 58.80(2)$ Å, $b = 4.90(1)$ Å, $c = 8.69(1)$ Å, and $\beta = 99.0(3)°$, with the same group C2/c as in the high temperature phase [22]. This lead us to collect data at temperatures below the phase transition, from 154 to 135 K. Unfortunately, the crystal did not pass the transition undegraded, as shown by broader and more anisotropic Bragg peaks, so only lattice parameters were refined using neutron data. The values found for parameter c, $c = 8.980(2)$ Å at 154 K, just below the transition, and $c = 8.954(6)$ Å at 135 K, are not easily reconciled with Enkelmann's value at 110 K, since all these data together would imply a contraction of 0.3 Å, or 3%, in less than 30 K. It was then decided to redetermine 3BCMU monomer crystal structure at 110 K by X-rays. The crystal is monoclinic, C2/c with $a = 58.715(2)$, $b = 4.8687(2)$, $c = 8.9578(3)$ Å, $\beta = 97.593(1)°$, $V = 2538.3(2)$ Å^3, $Z = 4$, $D_x = 1.257$ Mg m^{-3}, $\mu = 0.94$ cm^{-1}, $F(000) = 1032$. Crystal data, atomic positions, and bond lengths and angles are given on Tables 1–3. The lattice parameters obtained are in line with neutron data (see Table 4 and Fig. 1a–e). The filling factor is 0.69 at 110 K.

The main difference between [22] and our 110 K data concerns parameter **c**. However, there are also differences in the other ones that are larger than combined stated uncertainties: 0.04(1) Å on **b**, 0.10(2) Å on **a** and 1.4(3)° on $\boldsymbol{\beta}$. These differences might be due to a phase transition very near 110 K, the structure found in [22] then corresponding to a new lower temperature phase. To check this, the crystal structure was determined at 93 and 120 K, and as shown in Fig. 1a–e and Table 4, no such phase change is observed. The discrepancy should therefore be ascribed to polymorphism. However, the bond lengths and angles in the two structures are very similar, the only significant differences (up to 4° or 0.03 Å) concerning the N atom, that is the region of the hydrogen bond.

3.4. The phase transition

The X-ray 110 K molecular structure and the neutron 270 K one are very similar; the main difference lies in the CC bond lengths in the terminal butyl group. This may be due to poor statistics since the neutron scattering cross-section of a CH_2 group is very small. Also the butyl group are flexible, so disorder is possible at high temperature. The phase transition thus corresponds to changes in the packing of the molecules rather than in their conformation.

At the transition, discontinuous jumps are observed for **a** ($\Delta\mathbf{a} \approx 0.6$ Å), and for $\boldsymbol{\beta}$ ($\Delta\boldsymbol{\beta} \approx 3°$); **b** very slightly increases by 0.01 Å to 4.875 Å, and parameter **c** and the volume seem to be continuous. The decrease of **a** seems related to closer packing of neighbouring lamellae: the distance between terminal C12 carbons on either side of the interlamellar space decreases by 0.5 Å between 270 and 100 K, corresponding to closer contact of the terminal methyl groups.

This indicates that the transition corresponds essentially to a lateral shift of neighbouring lamellae, which continues down to 120 K (change of $\boldsymbol{\beta}$). A similar situation where a second order transition is superseded, before completion, by a weak first order one, is also observed in another diacetylene crystal, pTS, near 160 K [37].

3.5. Hydrogen bonds

The geometry of the H-bond at 270 K is shown in Scheme 4. The N···O distance is 2.89 Å, the N–H bond length is 1.05 Å and the three atoms are nearly collinear (NHO angle is 175°). The HOC angle is 165°. At 110 K, the exact position of H is not known, but N···O is 2.85 Å. The repeat distances are 4.878 Å at 270 K and 4.869 Å at 110 K. Therefore, it is likely that the H-bond strengths are nearly identical at the two temperatures, and presumably independent of T. This is consistent with the small temperature dependence of parameter b.

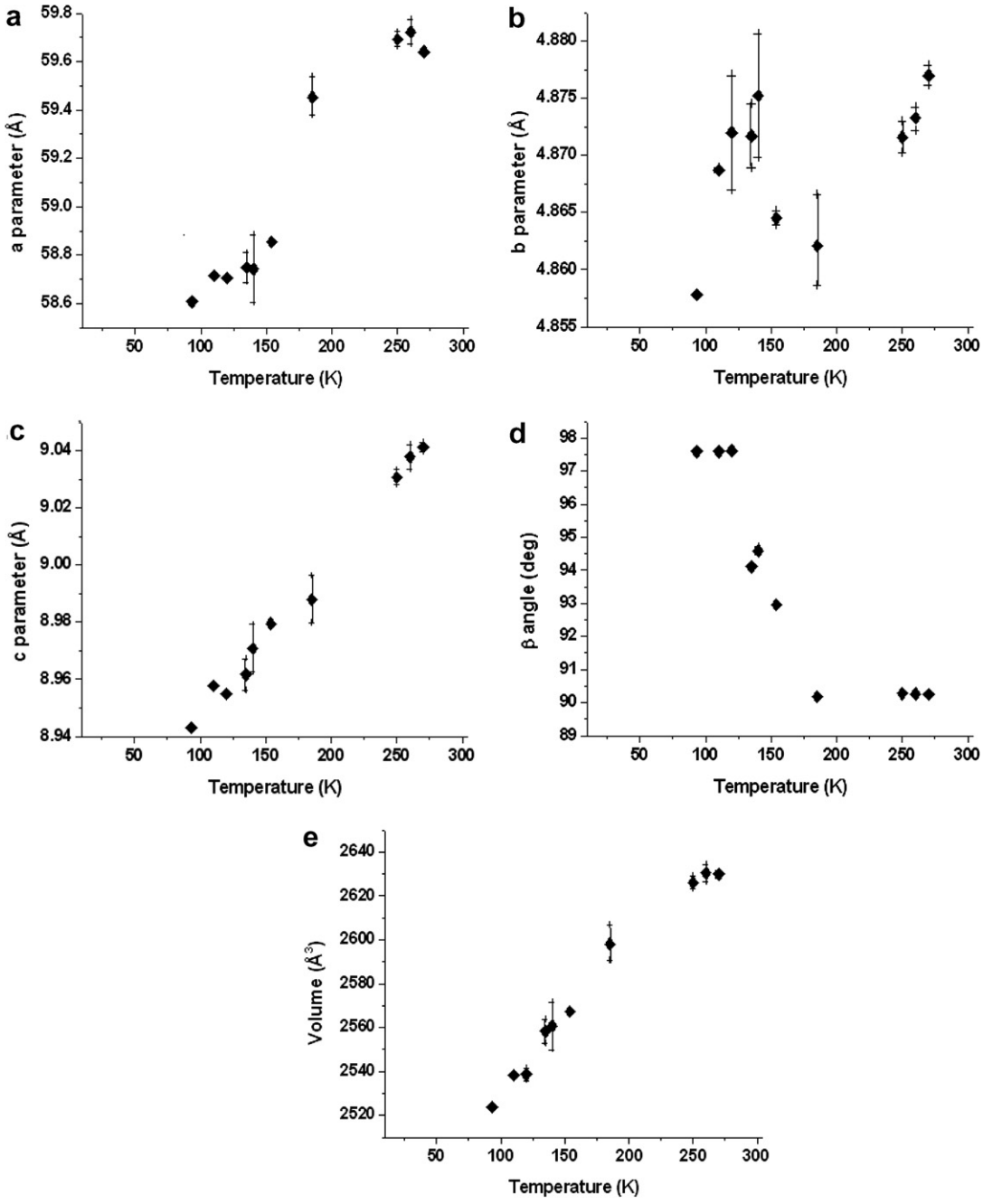

Fig. 1. (a–e) Temperature dependence of the 3BCMU monomer crystal unit cell. Errors bars are shown only for points where they are larger than the symbol size. (a) **a** Parameter in Å; (b) **b** parameter in Å, -note that the whole ordinate range is only 2.5×10^{-2} Å; (c) **c** parameter in Å; (d) $\boldsymbol{\beta}$ angle in degrees; (e) unit cell volume in $Å^3$.

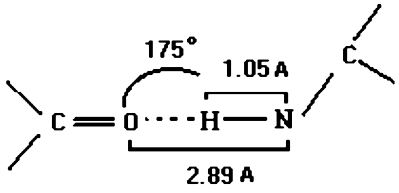

Scheme 4. Geometry of the H-bond in 3BCMU monomer at 270 K.

This bond is moderately strong in the classification by Steiner [38]. Its geometry is close to that of the average one in polypeptides, where N···O is 2.8 Å and the repeat distance 4.88 Å. A statistical analysis by Gavezzotti and Filippini [39] leads to overall averages for N–H···O type bonds of 1.95(8) Å for H···O, 2.92(7) Å for N···O and 166(8)° for the NHO angle; these values are very close to the ones found in 3BCMU.

According to Steiner [38], moderately strong bonds have energies between 4 and 15 kcal/mol (170–650 meV/bond). In the case of urea, an average H-bond energy of 5.25 kcal/mol has been deduced from the experimental sub-

limation energy [40] and recent theoretical calculations agree [41]. H–O distances in the Urea crystal are about 2 Å. One can reasonably expect that the H-bond energy in 3BCMU is larger, say between 6 and 9 kcal/mol, or 0.25 to 0.4 eV/bond. This cannot be more than a conjecture at this stage, since bond energy does not necessarily vary monotonously with bond length [41].

4. 4BCMU monomer

It has been shown by Differential Scanning Calorimetry that 4BCMU monomer crystal exhibits two first order transitions at 226 K and 318K [1], separating 3 phases: phase I for $T < 226$ K, phase II for $225 < T < 318$ K and phase III for $318 < T < 345$ K which is the melting point of the monomer crystal.

In this paper we focus on phase I and phase II, because 4BCMU polymerization is usually performed at room temperature (in phase II) and physical studies are performed either at low temperature (in phase I), or in some cases at room temperature.

4.1. Phase II ($225 < T < 318$ K)

If all unit cell parameters are left free, angles α and β converge to 90.00 within the uncertainties, whereas $\gamma = 90.21(3)$. However, far too many systematic extinction rules are observed to agree with a monoclinic space group. The observed rules are: $h00$, $0k0$, $00l$: $2n$; $h0l$: $h = 2n$; $hk0$: $h = 2n$; hkl: $h + k = 2n$. Therefore, it was assumed that the structure is in fact orthorhombic. Considering the observed extinctions, the possible space groups are no. 36 $Cmc2_1$ (non-centrosymmetric) or no. 63 Cmcm (centrosymmetric). It was checked that second harmonic generation is absent in this crystal at room temperature.[1] Furthermore, none of the properties implied by group $Cmc2_1$ (a polar group, piezoelectric and optically active) has been observed in 4BCMU monomer. It is then concluded that Cmcm is the correct space group of 4BCMU in phase II. The unit cell contains 8 molecules with the 2 independent molecules on general positions. At room temperature (296 K), using 111 non-weak reflections, the orthorhombic cell dimensions are: $a = 109.26(4)$ Å, $b = 11.344(4)$ Å, $c = 4.813(1)$ Å, and the unit cell volume $V = 5965$ Å^3 with $Z = 8$. This is a quite open structure: the filling factor, calculated as for 3BCMU is only 0.64 at room temperature.

These values are identical, within the stated uncertainties, to those obtained from a refinement including γ, which are: $a = 109.24(4)$ Å, $b = 11.344(3)$ Å, $c = 4.813(1)$ Å and $\gamma = 90.21(3)°$.

[1] A powder containing $\leqslant 10^{-5}$ polymer in weight was irradiated at 1.06 μm. No signal was detected at 530 nm. The very weak two-photon excited fluorescence of the small amount of poly-4BCMU was easily detected at about 660 nm, although its quantum yield is $\approx 10^{-4}$ only [42]. Any possible SHG signal is more than 2 orders of magnitude smaller.

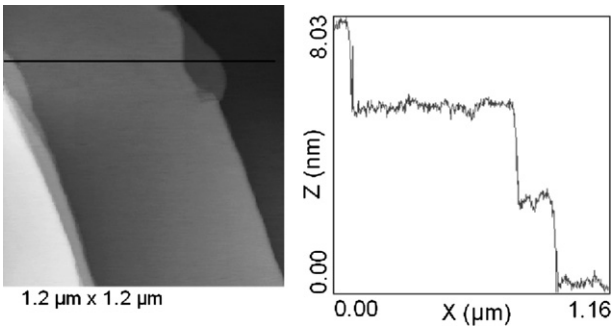

Fig. 2. AFM image of a 4BCMU monomer crystal surface. Image size 1.2×1.2 μm. A section along the dark line is shown. Three steps one lamella high (2.7 nm) are seen. 5.4 nm high steps (two lamellae) are present in other regions of the figure.

The 8 molecules are arranged in 4 lamellae, each ca 27.3 Å thick. 4BCMU monomer crystals show one well developed (100) face (platelet habit). This surface was studied by AFM in the tapping mode at room temperature. It shows atomically flat facets, separated by steps typically 1 to several μm apart (Fig. 2). The most common step heights are close to 27 Å and 54 Å. The slight observed deviation from these values are due to uncertainties in z range calibration. Occasionally, heights of ca 82 Å or more were observed. This indicates that the important structural unit within the crystal is indeed the lamella. As in most lamellar structures, the occurrence of stacking faults is to be expected.

It was sometimes possible to observe on a facet periods of ca 4.7 ± 0.2 and 12 ± 1 Å at right angle to one another, corresponding to the **b** and **c** unit cell dimensions. The monomer crystal is, however, easily damaged by the tip, in the experimental conditions required to observed these periodicities.

The temperature dependence of the unit cell parameters is shown in Fig. 3a–e and Table 5. The thermal expansion coefficients, deduced from these graphs, are:

in the a direction $\alpha_a \approx 3.4 \pm 3 \times 10^{-6}$ K^{-1}compatible with zero,
in the b direction $\alpha_b \approx 4.9 \pm 0.5 \times 10^{-5}$ K^{-1},
in the c direction $\alpha_c \approx 6.1 \pm 0.5 \times 10^{-5}$ K^{-1}.

There is only one previous structural investigation of 4BCMU monomer [43], based on powder X-ray diffraction at room temperature. The proposed space group is orthorhombic, possibly $P2_12_12$, with $a = 53.77(6)$ Å, $b = 11.34(2)$ Å, $c = 4.871(5)$ Å based on 18 reflections only.

These results differ from the present ones mainly on two points: the **a** parameter is halved so the unit cell is primitive, and **c** is significantly larger, by more than 1%. A centred cell is made necessary in our structure by the extinctions observed, and the $(h11)$ reflections cannot be properly indexed otherwise; the first difference between [43] and the present results may then only reflect the limited amount of experimental information collected by these

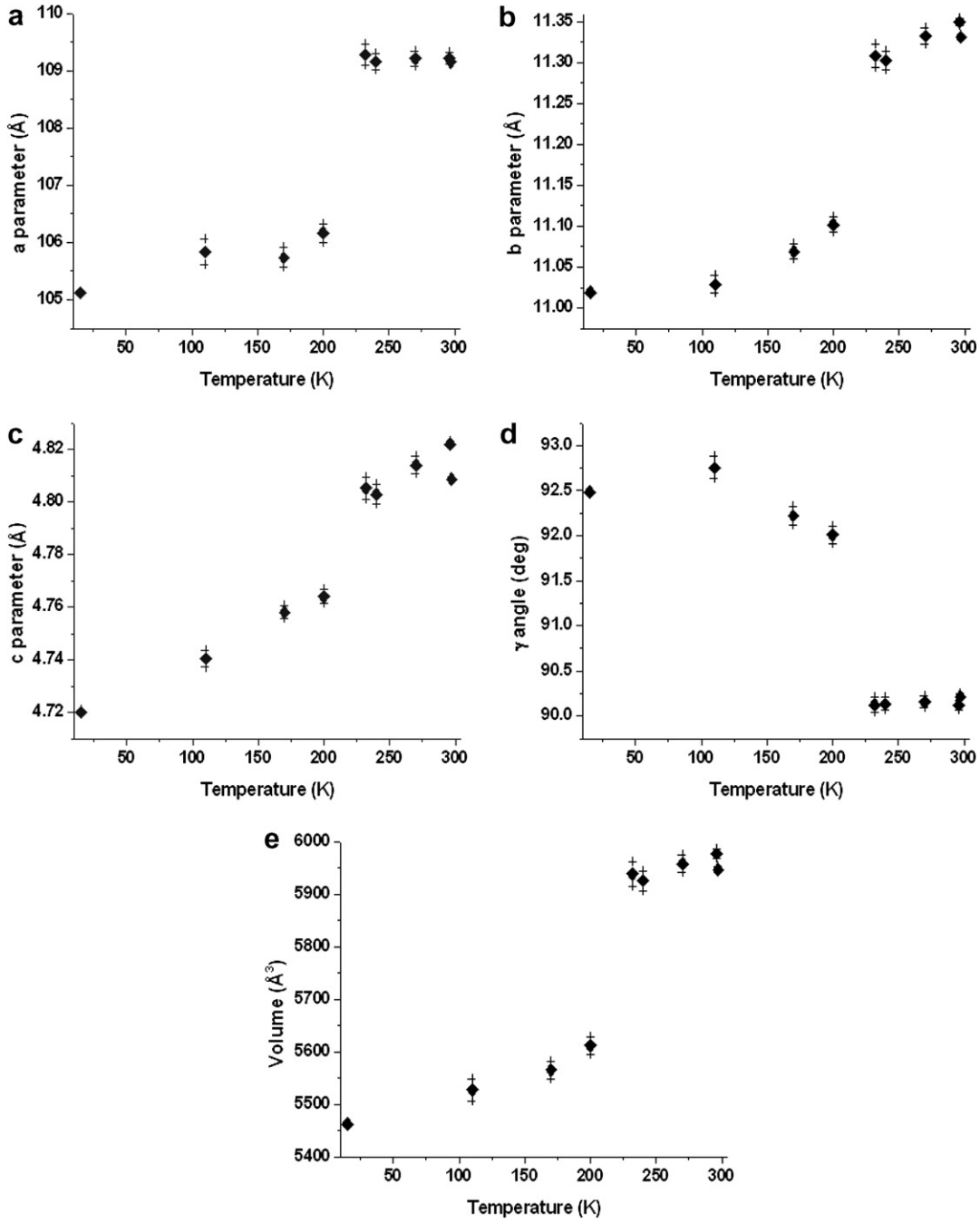

Fig. 3. (a–e) Temperature dependence of the 4BCMU monomer crystal unit cell: (a) **a** parameter in Å; (b) **b** parameter in Å; (c) **c** parameter in Å; (d) γ angle in degrees; (e) unit cell volume in Å^3.

authors. The second discrepancy has a different origin: 4BCMU monomer is extremely reactive under X- or γ-ray irradiation. A 3000 Rad γ-ray dose produces 10% polymer in weight in a single crystal at room temperature [8]. Powders are very reactive as well, although less by a factor 5–10 depending on grain size and perfection [8,19]. It is then likely that the sample studied in [43] had a significant polymer content. Moreover DSC experiments (Fig. 4) show that the monomer thermodynamic properties are already affected at a polymer content slightly larger than 2% in weight.

All monomer crystals used in the present study contained less than 2% polymer chains in weight as checked spectroscopically [8]. Comparison of measurements taken at a polymer content $x_p < 10^{-4}$ in weight, as typically used in spectroscopic experiments, and at $x_p \approx 2\%$, show that the presence of polymer chains does not significantly affect the unit cell dimensions. The values reported here are therefore representative of the ''pure monomer'' limit.

Above ~10% polymer, we have observed that the lamellae stacking becomes disordered. Apparently, this disorder persists in the pure polymer [44]. In the most detailed crys-

Table 5
4BCMU temperature dependence of lattice parameters

Temperature (K)	a (Å)	b (Å)	c (Å)	γ (°)	V (Å^3)
15	105.12(2)	11.0191(14)	4.7202(5)	92.48(13)	5463(3)
110	105.8(2)	11.029(11)	4.7404(32)	92.75(12)	5527(21)
170	105.74(18)	11.069(9)	4.7580(25)	92.22(10)	5565(17)
200	106.17(16)	11.102(9)	4.7639(26)	92.01(9)	5612(16)
232	109.28(18)	11.308(14)	4.8052(43)	90.13(8)	5938(22)
240	109.15(15)	11.303(11)	4.8028(38)	90.14(7)	5925(19)
270	109.21(13)	11.332(10)	4.8140(34)	90.16(6)	5957(17)
296	109.22(10)	11.349(5)	4.8219(12)	90.12(5)	5977(9)
297	109.15(4)	11.331(3)	4.8087(8)	90.22(3)	5947(4)

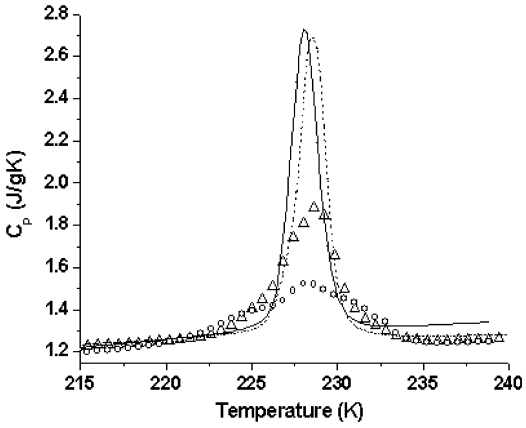

Fig. 4. DSC scan of the 4BCMU low temperature phase transition as a function of polymer content: solid line pure monomer crystal, dotted line 0.7% polymer, open triangles 1.4% and open circles 2%, in weight.

tallographic investigation of poly-4BCMU [45], *hkl* reflections are reported to be very diffuse; no *hkl* and only 43 *hk0* reflections could be recorded. The determined structure is orthorhombic with $a = 53.75(2)$ Å, $b = 10.997(3)$ Å, $c = 4.880(5)$ Å, $Z = 4$, proposed group no. 57, Pmab. This **c** value is very close to the values found in other PDA, which range between 4.88 and 4.91 Å [5]. Note that group Cmcm we propose for the monomer is a minimal isomorphic supergroup of group no. 57. It is likely that, apart from the observed disordering, which may probably be described as a multiplication of stacking faults, there is no other major structural change while going from monomer to polymer at least at room temperature.

4.2. Phase I ($T < 226$ K)

The unit cell, determined with 360 non-weak reflections, is monoclinic with $Z = 8$ molecules. The proposed group is P1c1 no. 7 (centrosymmetric) or P12/*c*1 no. 13 (non-centrosymmetric). As discussed for phase II the former one is preferred. At 15 K the unit cell parameters are: $a = 105.12(2)$ Å, $b = 11.019(3)$ Å, $c = 4.7202(5)$ Å, $\gamma = 92.48(1)$ and $V = 5462(3)$ Å^3, corresponding to a filling factor of 0.67. Their temperature dependences are shown in Fig. 3a–e. The thermal expansion coefficients above about 100 K are:

in the **a** direction $\alpha_a \approx 1.64 \pm 0.03 \times 10^{-5}\,\mathrm{K}^{-1}$,
in the **b** direction the variation is not linear $\alpha_b \approx 8.3 \pm 0.2 \times 10^{-5}\,\mathrm{K}^{-1}$ between 160 K and 220 K and almost zero below,
in the **c** direction it is almost the same that in phase I: $\alpha_c \approx 6 \pm 0.2 \times 10^{-5}\,\mathrm{K}^{-1}$.

Below $T = 100$ K the temperature dependences become weaker.

4.3. Phase transition between I and II

At the phase transition lamellae slide along the ac plane, together with an important decrease of the unit cell dimensions and volume; this decrease is of 0.6% in the *c* direction, 1.4% in the *b* direction and 2.4% in the *a* direction, so the volume shrinks by 4.7% (Fig. 3a–e and Table 5). Nevertheless the crystal does not break, and there is no detectable degradation of the Bragg peaks lineshape. This behaviour may be explained, at least in a part, by a new organization of the C_4H_9 at the end of the side group.

5. Conclusion

The two materials studied here belong to a family of DA which side-groups are linked in the crystal by chains of Hydrogen bonds running parallel to the polymer chain growth direction. The corresponding repeat distance is often close to 4.9 Å [39], so when this distance dominates the molecular packing, the resulting crystal is – as is the case of 3BCMU and 4BCMU – highly reactive under γ-ray irradiation (although always thermally inactive). Consequently, X-ray crystal structure determinations can only be performed at low temperature, where the structure may differ from the room T phase in which polymerisation is performed.

This is the case of 3BCMU. The 270 K structure obtained here is therefore the first of its kind. The relative orientation and distance of the reactive C4 groups correspond well to the reactivity criteria which have been proposed [4,5]. The only other room temperature complete structure of a reactive DA with H-bonds is a polymorph of TCDU, a DA with side group $–(CH_2)_4–OCONHC_6H_5$

[46]. This DA is rather unreactive, a γ-ray dose of 60 MRad did not polymerize it completely. Two other slightly more reactive polymorphs of TCDU were studied at 120 K [47a,47b]. In all these structures, the unit cell parameters along the chain growth direction are much larger than in 3BCMU: between 5.11 and more than 5.23 A. So, the geometry is indeed much less favourable to polymerization.

The present structure was obtained by neutron diffraction, allowing Hydrogen atomic positions to be determined; the complete geometry of the H-bonds has been obtained, and is typical of medium strength H-bonds, so an approximate value of its energy can be inferred [38]. This is relevant to the photoreactivity of 3BCMU and 4BCMU, discussed in [24].

The temperature dependences of unit cell parameters of 3BCMU and 4BCMU have been measured. They show that isolated poly-3BCMU chains are practically unstrained in their monomer crystal matrix at all temperatures. Such chains are indeed good models for the chains in bulk PDA crystals, in which the chains are assumed to be unstrained.

Poly-4BCMU chains are always under compression in their monomer crystal, and the more so the lower T. The very small exciton absorption broadening [1] shows that isolated polymer chains remain also in register, despite a longitudinal compression of 3% at low temperature. This allows study of electronic properties of PDA in usually inaccessible conformations, see [25]. Indeed, the exciton energy and vibrational frequencies of these chains vary with T in an uncommon way.

The two crystals have lamellar structures. The minimum distance between diacetylene groups belonging to neighbouring lamellae is 27 Å, so their interaction is negligible. These groups actually form a 2D crystal, as far as electronic properties (such as energy transfer) are concerned. Similarly, electronic interaction between polymer chains belonging to different lamellae is always negligible. This does not mean that the 3D packing of the lamellae is irrelevant, since the conformation of side groups may affect the chain geometry, hence its electronic structure [48].

Stacking faults are likely to occur in such lamellar structures. Since the interaction between side groups on either side of such a fault are not identical to that in the perfect crystal, chains belonging to lamellae nearby a stacking fault may have slightly different electronic structures, hence absorption spectra. Spectra of such chains, slightly different from that of the main population of chains, are indeed observed [1].

Supplementary data

CCDC 297777 and 635004 contain the supplementary crystallographic data, respectively, for 3BCMU at 110 K by X-ray diffraction and 3BCMU at 270 K by neutron diffraction. These data can be obtained free of charge via www.ccdc.cam.ac.uk/data_request/cif, or by emailing-data_request@ccdc.cam.ac.uk, or by contacting The Cambridge Crystallographic Data Centre, 12, Union Road, Cambridge CB2 1EZ, UK; fax: +44 1223 336033.

Acknowledgements

We thank ILL for beam time allocated on D19, Dr. P. Langan and Dr. S. Mason at ILL for their assistance in data collection and useful discussions, Dr. B. Suchod for her help in crystallographic data processing, Dr. J. Berréhar for growing crystals and for DSC experiments, Dr. T. Barisien for help in acquiring AFM images, and Pr I. Ledoux-Rak to have shown that no second harmonic generation is present in 4BCMU crystals.

Appendix. Microscopic evidence of the lattice mismatch between 4BCMU and poly-4BCMU

The consequences of lattice mismatch at room temperature between 4BCMU and poly-4BCMU are visible on a macroscopic scale in polymer single crystal films grown at the surface of 4BCMU monomer. Electron beam polymerization of a monomer crystal creates a thin polymer

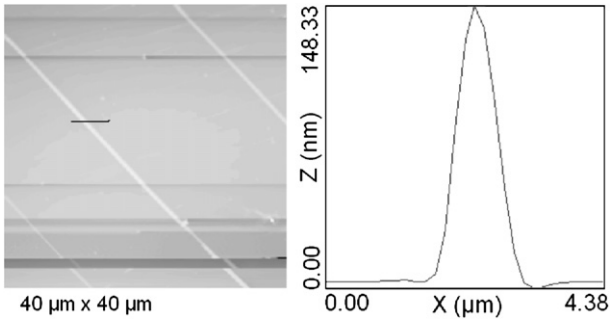

Fig. 5. AFM image of the surface of a poly-4BCMU thin film on its monomer crystal. Film thickness ~250 nm. The straight lines are ridge running perpendicular to the chain direction. The section shows a ridge profile: height is 150 nm, width 1 μm.

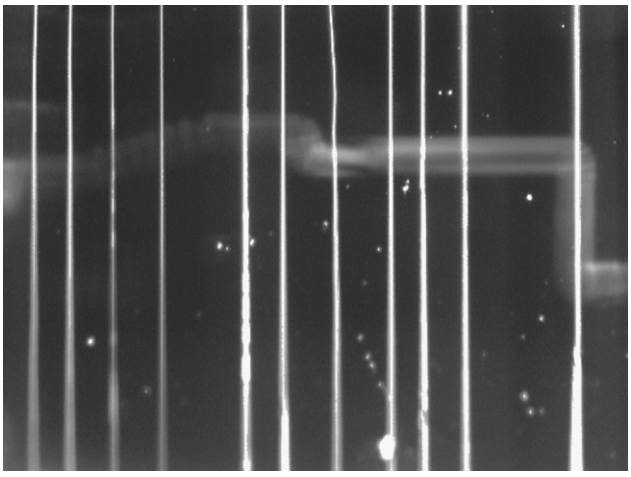

Fig. 6. Optical microscope image, in grazing light, of a 4BCMU polymer film on its monomer substrate, $750 \times 570\ \mu m^2$.

surface layer on the underlying monomer substrate. This polymerisation proceeds epitaxially and leads to a thin crystalline polymer film as described elsewhere [49,50]. Fig. 5 shows an AFM image of a 4BCMU thin film on its monomer substrate. The white lines on the picture are perpendicular to the chains direction; they correspond to ridges having a width between 1 and 2.5 μm and a height between 100 and 250 nm comparable to the film thickness. Fig. 6 shows a larger scale optical microscope image taken in grazing light. An almost regular pattern of ridges can be seen. The polymer film relaxes at least part of the compressive strain along the *c* direction via the creation of these ridges which increase the film length in that direction. The ridges presumably correspond to delamination of the film via fracture at the monomer-polymer interface.

References

[1] S. Spagnoli, J. Berréhar, C. Lapersonne-Meyer, M. Schott, J. Chem. Phys. 100 (1994) 6195.
[2] G. Wegner, Z. Naturforsch. 24b (1969) 824.
[3] M.D. Cohen, G.M.J. Schmidt, J. Chem. Soc. (1964) 1996.
[4] R.H. Baughman, K.C. Yee, J. Polym. Sci. Macromol. Rev. 13 (1978) 219.
[5] V. Enkelmann, Adv. Polym. Sci. 63 (1984) 91.
[6] C. Lapersonne-Meyer, J. Berréhar, M. Schott, S. Spagnoli, Mol. Cryst. Liq. Cryst. 256 (1994) 423.
[7] T. Barisien, L. Legrand, M. Schott, in preparation.
[8] S. Spagnoli, J. Berréhar, C. Lapersonne-Meyer, M. Schott, A. Rameau, M. Rawiso, Macromolecules 29 (1996) 5615.
[9] B. Kraabel, D. Hulin, C. Aslangul, C. Lapersonne-Meyer, M. Schott, Chem. Phys. 289 (1998) 83.
[10] B. Kraabel, M. Joffre, C. Lapersonne-Meyer, M. Schott, Phys. Rev. B 58 (1998) 15777.
[11] S. Haacke, J. Berréhar, C. Lapersonne-Meyer, M. Schott, Chem. Phys. Lett. 308 (1999) 363.
[12] R. Lécuiller, J. Berréhar, C. Lapersonne-Meyer, M. Schott, Phys. Rev. Lett. (1998) 4068.
[13] R. Lécuiller, J. Berréhar, J.D. Ganière, C. Lapersonne-Meyer, P. Lavallard, M. Schott, Phys. Rev. B 66 (2002) 125205.
[14] T. Guillet, J. Berréhar, R. Grousson, J. Kovensky, C. Lapersonne-Meyer, M. Schott, V. Voliotis, Phys. Rev. Lett. 87 (2001) 087401.
[15] F. Dubin, J. Berréhar, R. Grousson, T. Guillet, C. Lapersonne-Meyer, M. Schott, V. Voliotis, Phys. Rev. B 66 (2002) 113202.
[16] F. Dubin, R. Melet, T. Barisien, R. Grousson, L. Legrand, M. Schott, V. Voliotis, Nature Phys. 2 (2006) 32.
[17] M. Schott, in: G. Lanzani (Ed.), Photophysics of Molecular Materials, Wiley-VCH, Weinheim, 2006, p. 49.
[18] F. Dubin, J. Berréhar, R. Grousson, M. Schott, V. Voliotis, Phys. Rev. B 73 (2006) 1213021.
[19] G.N. Patel, Radiat. Phys. Chem. 18 (1981) 913.
[20] H. Sixl, Adv. Polym. Sci. 63 (1984) 49.
[21] J.P. Aimé, J. Lefebvre, M. Bertault, M. Schott, J.O. Williams, J. Phys. Fr. 43 (1982) 307.
[22] V. Enkelmann, G. Wenz, M.A. Müller, M. Schmidt, G. Wegner, Mol. Cryst. Liq. Cryst. 105 (1984) 11.
[23] J.P. Aimé, M. Schott, M. Bertault, L. Toupet, Acta Crystallogr. B 44 (1988) 617.
[24] M. Schott, S. Spagnoli, G. Weiser, Chem. Phys. 333 (2007) 246.
[25] S. Spagnoli, J. Berréhar, J.P. Fave, M. Schott, Chem. Phys. 333 (2007) 254.
[26] G.J. McIntyre, Neutron Synchrotron Radiat. Condens. Matter Stud. 1 (1993) 179.
[27] Z. Otwinowski, W. Minor, in: C.W. Carter, R.M. Sweet (Eds.), Methods in Enzymology, Macromolecular Crystallography, Part A, vol. 276., Academic Press, London, 1997, p. 307.
[28] Nonius Kappa CCD Software, Nonius BV, Delft, 1999.
[29] A. Altomare, M.C. Burla, M. Camalli, G. Cascarano, C. Giacovazzo, A. Guagliardi, A.G.G. Moliterni, G. Polidori, R. Spagna, J. Appl. Crystallogr. 32 (1999) 115.
[30] G.M. Sheldrick, SHELX97, Goettingen University, Goettingen, 1997.
[31] A.J.C. Wilson, E. Prince (Eds.), International Tables for X-ray Crystallography, vol. C, Kluwer, Academic Publishers, Dordrecht, 1992.
[32] <http://www.accelrys.com/products/mstudio>.
[33] S.R. Hall, H.D. Flack, J.M. Stewart (Eds.), Xtal3.2 Reference Manual, Universities of Western Australia, Australia, and Maryland, USA, 1992.
[34] L.J. Farrugia, J. Appl. Crystallogr. 30 (1997) 565.
[35] A.L. Spek, J. Appl. Crystallogr. 36 (2003) 7.
[36] A.I. Kitaigorodskii, Organic Chemical Crystallography, Consultants Bureau, New York, 1961.
[37] (a) P. Robin, J.P. Pouget, R. Comes, A. Moradpour, J. Phys. 41 (1980) 415;
(b) M. Bertault, A. Collet, M. Schott, J. Phys. Lett. 42 (1981) L-131;
(c) J.P. Aimé, Ph.D. thesis, Université Paris 7, 1983.
[38] T. Steiner, Angew. Chem. Int. Ed. 41 (2002) 48.
[39] A. Gavezzotti, G. Filippini, J. Phys. Chem. 98 (1994) 4831.
[40] S. Swaminathan, B.M. Craven, R.K. McMullen, Acta Crystallogr. B 39 (1984) 300.
[41] C.A. Morrison, M.M. Siddick, Chem. Eur. J. 9 (2003) 628.
[42] R. Lécuiller, J. Berréhar, C. Lapersonne-Meyer, M. Schott, J.D. Ganière, Chem. Phys. Lett. 314 (1999) 255.
[43] C. Brouty, P. Spinat, M.C. Sichère, A. Whuler, Z. Kristallogr. 176 (1986) 13.
[44] Y. Takahashi, T. Zakoh, K. Inoue, H. Ohnuma, T. Kotaka, Synth. Met. 18 (1987) 423.
[45] C. Brouty, P. Spinat, A. Whuler, Acta Crystallogr. C 44 (1988) 1070.
[46] H. Tachibana, R. Kumai, N. Hosaka, Y. Tokura, Chem. Mater. 13 (2001) 155.
[47] (a) H. Gross, H. Sixl, C. Kroehnke, V. Enkelmann, Chem. Phys. 45 (1980) 15;
(b) V. Enkelmann, J. Chem. Res. 344 (1981) 3901.
[48] M. Schott, J. Phys. Chem. B 110 (2006) 15864.
[49] J. Berréhar, C. Lapersonne-Meyer, M. Schott, Appl. Phys. Lett. 48 (1996) 630.
[50] J. Berréhar, P. Hassenforder, C. Lapersonne-Meyer, M. Schott, Thin Solid Films 190 (1990) 181.